Paleobiology, 35(2), 2009, pp. 251–269

A biomechanical model of feeding kinematics for *Dunkleosteus terrelli* (Arthrodira, Placodermi)

Philip S. L. Anderson and Mark W. Westneat

Abstract.—Biomechanical models illustrate how the principles of physics and physiology determine function in organisms, allowing ecological inferences and functional predictions to be based on morphology. Dynamic lever and linkage models of the mechanisms of the jaw and skull during feeding in fishes predict function from morphology and have been used to compare the feeding biomechanics of diverse fish groups, including fossil taxa, and to test ideas in ecological morphology. Here we perform detailed computational modeling of the four-bar linkage mechanism in the skull and jaw systems of *Dunkleosteus terrelli*, using software that accepts landmark morphological data to simulate the movements and mechanics of the skull and jaws during prey capture. The linkage system is based on the quadrate and cranio-thoracic joints: Cranial elevation around the cranio-thoracic joint forces the quadrate joint forward, which, coupled with a jaw depressor muscle connecting the jaw to the thoracic shield, causes the jaw to rotate downward during skull expansion. Results show a high speed transmission for jaw opening, producing a rapid expansion phase similar to that in modern fishes that use suction during prey capture. During jaw closing, the model computes jaw and skull rotation and a series of mechanical metrics including effective mechanical advantage of the jaw lever and kinematic transmission of the skull linkage system. Estimates of muscle cross-sectional area based on the largest of five specimens analyzed allow the bite force and strike speed to be estimated. Jaw-closing muscles of *Dunkleosteus* powered an extraordinarily strong bite, with an estimated maximal bite force of over 6000 N at the jaw tip and more than 7400 N at the rear dental plates, for a large individual (10 m total length). This bite force capability is among the most powerful bites in animals. The combination of rapid gape expansion and powerful bite meant that *Dunkleosteus terrelli* could both catch elusive prey and penetrate protective armor, allowing this apex predator to potentially eat anything in its ecosystem, including other placoderms.

*Philip S. L. Anderson.** *Department of Geophysical Sciences, University of Chicago, Chicago, Illinois 60637*
Mark W. Westneat. *Department of Zoology, Field Museum of Natural History, Chicago, Illinois 60605*
*Present address: *Department of Earth Sciences, University of Bristol, Wills Memorial Building, Queen's Road, Bristol BS8 1RJ, United Kingdom. E-mail: Phil.Anderson@bristol.ac.uk*

Accepted: 25 November 2008

Introduction

A major challenge in paleobiology is the reconstruction of biological function in extinct organisms, which cannot be directly observed. Often, the possible function of a fossil morphology is based on similarity with modern structures, be they homologous structures (Cowan 1979; Witmer 1995), analogous biological structures (Stanley 1970; Radinsky 1987; Labandeira 1997) or analogies to man-made structures (Cowan 1975; Myhrvold and Currie 1997). Functional morphology based on comparisons with homologous structures in closely related taxa is referred to as historical (phylogenetic) comparison (Lauder 1995; Weishampel 1995; Ross 1999). Extant phylogenetic bracketing (Witmer 1995) is a historical method that compares the fossil organism with two extant sister lineages to validate functional hypotheses. However, the more distantly related the taxa, or more detailed the comparison, the less useful this method becomes (Plotnick and Baumiller 2000). Older fossil taxa (particularly from the Paleozoic) show unique morphologies that are not readily comparable to anything seen in the modern animal kingdom (Coates and Sequeira 1998). Furthermore, the bracketing method falls short when the functional structure being examined first appears in the study group. An alternative is the ahistorical (paradigmatic) approach, which focuses on the specific morphological structures of the taxa in question (DeMar 1976; Lauder 1995; Ross 1999). This method often relies on comparisons with biological or mechanical analogies.

Identification of an analogue for a fossil form needs to be tested, commonly done by defining

© 2009 The Paleontological Society. All rights reserved. 0094-8373/09/3502-0005/$1.00

an optimum structure or ''paradigm'' to compare with the fossil (Rudwick 1964; Ross 1999). Once a possible function is hypothesized for a given fossil structure, the optimum structure for that function (based on engineering and the nature of the biological materials in question) can be predicted. The degree to which the fossil structure is similar in form to the ''paradigm'' is the test of the hypothesized function. The test often can be subjective, based on visual comparison of the fossil and paradigm, although quantitative methods have become more common (Ashley-Ross and Gillis 2002; Gaudin et al. 2006). This method also assumes that a single optimum form exists for a given function, as opposed to the more likely scenario of there being several local optima (Signor 1982; Alexander 1996). Furthermore, the paradigm method assumes that the organism can achieve a theoretical optimum for a particular function, neglecting developmental constraints, historical contingency, and functional trade-offs, all of which can result in suboptimal form (Gould and Lewontin 1979; Niklas 1994; Seilacher and LaBarbera 1995; Plotnick and Baumiller 2000; Gould 2002). Methods of functional analysis based on homology and/or analogy offer a good source of hypotheses for function. However, a quantitative method of testing that allows for suboptimality is needed to evaluate these hypotheses. Recent analyses have eliminated some of these issues by statistically comparing a fossil taxon with a modern system considered an exemplar for a particular function (Shockey et al. 2007). While offering several insights into the possible functional morphology of fossil groups, this method still evaluates fossil forms based on modern behaviors as opposed to testing actual mechanics.

In this paper, we take a paleobiomechanical approach to functional analysis. Whereas the previous methods of functional analysis focus on overall similarity between fossil and modern structures, paleobiomechanics focuses more on specific similarities, which often come from basic inescapable rules of physics (Vogel 1998). Fundamentally, the field of biomechanics examines the relationship between biological form and structure in the context of physical laws and processes (Wainwright et al. 1976). Paleobiomechanics is the uniformitarian extension of biomechanical methodology (Alexander 1989). The basic laws of physics have not changed over the last 500 Myr. The same principles of lift and drag necessary to understand the flight of a bird can be applied to inferring pterosaur flight (Padian 1991). However, fossil taxa cannot be directly observed; therefore paleobiomechanics must rely heavily on biomechanical models to aid in inferring and testing mechanical consequences of form.

Biomechanical models attempt to represent the reality of biological systems, materials, or behaviors by reducing complex actions into simple relationships, using mathematics and physical laws (Nigg 1994). These models can be used to make predictions of behaviors that cannot be observed or to describe theoretical situations not yet observed. Paleontologists use biomechanical models based on modern experimental data to make predictions of how extinct species may have functioned. Blob (2001) derived a biomechanical model of posture related to changes in limb bone stress for fossil tetrapods. The model incorporated experimental data from force platform and bone stress experiments in modern iguanas and alligators (Blob 1998; Blob and Biewener 1999, 2001) and morphological data from fossil therapsids (mammal-like reptiles) (Blob 2001). The model shows that multiple postures were biomechanically plausible in therapsids. The model also led to insights into how principal limb bone stresses may have changed through evolution (Blob 2001). More recently, Gatesy and Baier (2005) used modern experimental data taken from motion analysis on avian flight to identify six kinetic components to the avian flight stroke that control trajectory. Combining this with kinematic data from both modern and fossil groups, Gatesy and Baier (2005) were able to develop criteria for testing hypotheses of flight origin in theropods. Biomechanical models have also been used to examine aspects of feeding behavior in fossil taxa, such as prey capture (Bellwood 2003; Kammerer et al. 2006).

Studies of the feeding mechanics of modern fishes have greatly benefited from the use of biomechanical models derived from engineering theory (reviewed in Westneat 2006). Sev-

eral studies on vertebrate feeding mechanics treat the mandible as a third-order lever (Barel 1983) and show that mechanical advantage values based on these lever mechanics in fish correlate highly with preferred prey type (Westneat 1994; Wainwright and Richard 1995). Recent studies have applied mechanical advantage analyses to fossil gars (Kammerer et al. 2006) and the evolution of herbivory in fishes (Bellwood 2003). Researchers have also identified more complex four-bar linkage mechanisms in the opercular (Anker 1974; Aerts et al. 1987; Durie and Turingan 2004), hyoid (Muller 1987, 1989), and oral jaw (Westneat 1990, 2004) systems of modern fish taxa. Westneat (1990) modeled both the oral jaw and hyoid systems in teleost fishes as four-bar linkage mechanisms and showed that the linkage models were highly accurate in predicting the kinematics of the jaw mechanisms. These models have since been modified and improved to include aspects of muscle physiology (Westneat 2003). The application of four-bar linkage modeling has recently been extended to the skull mechanics of *Dunkleosteus terrelli*, a fossil placoderm (Anderson and Westneat 2007).

Placoderms are a class of basal gnathostomes known from the Silurian and Devonian Periods (Benton 2005) and characterized by two-part dermal bony armor that covers the head and the anterior portion of the trunk (Denison 1978). Placoderms are an important group in early gnathostome evolution because most phylogenies place them as the earliest jawed vertebrate clade, sister to the chondrichthyan-osteichthyan split (Goujet 2001; Trinajstic and Hazelton 2007; con Zhu and Schultze 2001). A recent phylogenetic analysis of early gnathostomes has split placoderms into a series of stem gnathostome groups, with the order arthrodira (including *Dunkleosteus*) falling just outside crown Gnathostomata (Brazeau 2009). This phylogenetic placement, coupled with remarkable morphological variation in the feeding system (Carr 1995), makes placoderms an early example of jaw diversification that occurred in parallel to the diversification of crown gnathostomes. Therefore, arthrodire placoderms are an ideal clade for comparisons with functional diversification in modern fishes, thus offering a natural experiment in jaw design independent of the osteichthyan/chondrichthyan clade. *Dunkleosteus terrelli* (Newberry 1873) is one of the largest placoderm species known and is represented by several full skull and thoracic armor specimens (Fig. 1A). Miles (1969) described a feeding mechanism in arthrodire placoderms that included both jaw depression and cranial elevation driven by four muscle blocks. Miles (1969) also offered hypotheses for the feeding behavior of several specific taxa including *Dunkleosteus*, which he considers a slow-moving predator with a powerful bite.

In a recent analysis (Anderson and Westneat 2007), we proposed a biomechanical feeding model for *Dunkleosteus terrelli* based on a novel four-bar linkage mechanism, and calculated mechanical metrics including mechanical advantage, kinematic transmission, and bite force. Results of that study showed that *Dunkleosteus terrelli* combined a rapid gape expansion with a powerful bite, a combination not often seen in modern fish. These results are based on certain assumptions about the force and speed produced by the muscles. This study expands on this model, exploring these assumptions regarding muscle mechanics and other aspects of the model. The primary goals of this study are to (1) present the anatomical and biomechanical basis for the linkage model of *Dunkleosteus* in detail, (2) perform a wide range of simulations using alternative muscle conditions to establish confidence limits on estimates of bite speed and force, and (3) explore the utility of the linkage model by assessing levels of muscle strain, transmission of force and motion, and the range of placoderm jaw rotation in comparison to living fishes.

Methods

Specimens and Imaging

We measured five articulated (skull and thoracic armor) specimens of *Dunkleosteus terrelli* for use in the computer simulation. All specimens were obtained from the Cleveland Museum of Natural History (CM6090, CM7054, CM7424, CM5768, CM6194). Fragmented and individual plate remains were ex-

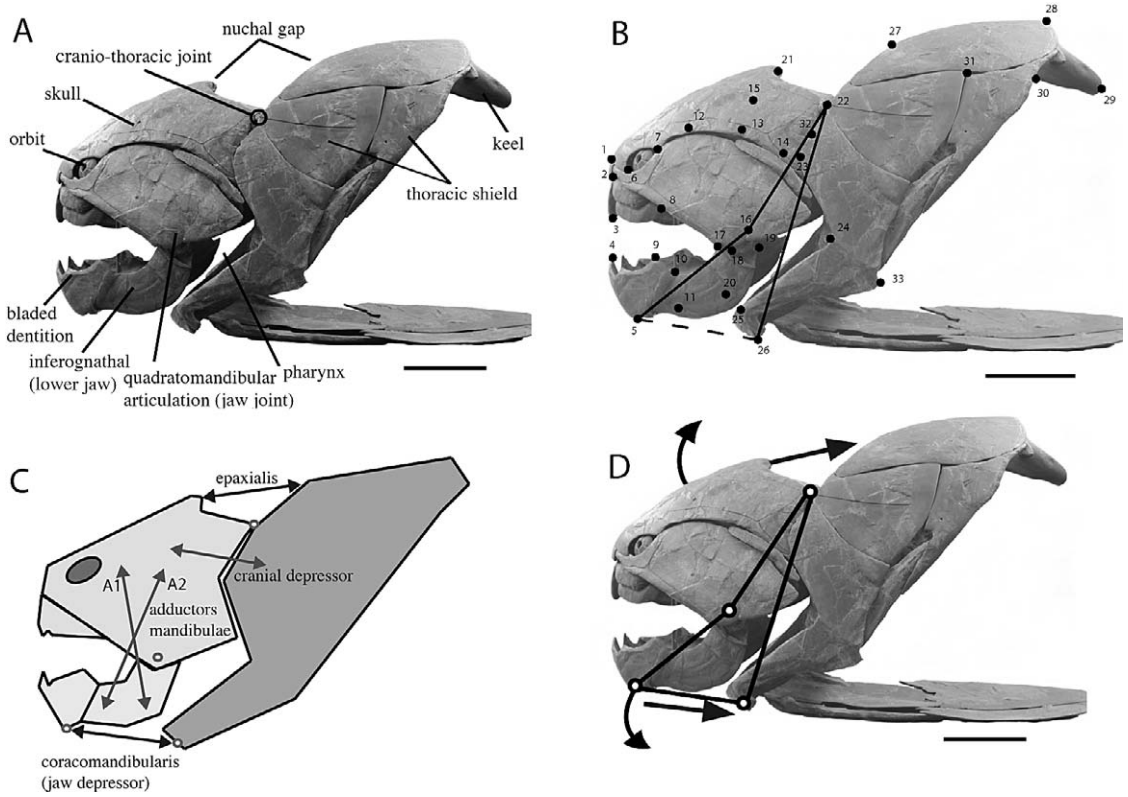

FIGURE 1. Anatomy and biomechanical model of the armored skull and thoracic region of *Dunkleosteus terrelli*. A, Anatomy of *Dunkleosteus terrelli*. B, Thirty-three morphological landmarks used in this study. They outline the four-bar linkage, muscle reconstructions and general shape of the skull and thoracic shield in *Dunkleosteus*. C, Drawing of (A) showing the four rotational joints (open circles) forming the four-bar linkage that mediates skull and mandibular rotation. The lines of action of four muscles are shown, including two jaw openers (epaxialis and coracomandibularis in black) and two jaw closers (cranial depressor and two alternate reconstructions of the adductor mandibulae in gray, labeled A1 and A2). D, Four-bar linkage motion during opening driven by EP and CM muscles. Scale, 20 cm. Specimen no. CM6090. Cleveland Museum of Natural History, Cleveland. (Figure modified from Anderson and Westneat 2007.)

amined to confirm and validate muscle reconstructions. Specimen CM5768 was used to obtain estimates of muscle volume and cross-sectional area for force measurements. Digital photographs of the five *Dunkleosteus* skulls were taken with a Nikon D70 SLR camera with a Nikkor 18–70 mm lens. The images were taken at maximum resolution: 3008 × 2000 pixels. These images were used to digitize 33 morphological landmarks from a left lateral view.

The Four-bar Linkage in *Dunkleosteus*

The head, jaws and pectoral girdle of *Dunkleosteus terrelli* are made of numerous interlocking plates, which often disarticulate after death (Fig. 1A). Articulated specimens found in the Cleveland Shale in Ohio, as well as similar species found in the Gogo Formation of Western Australia, help to reconstruct the plates into life position. The extensive flat overlapping surfaces along with a distinct lack of many jointed connections indicate that this species did not have many moving parts. Some movement along the overlapping portions might have been possible, especially in the cheek area during breathing and maybe even jaw opening (Long 1995). However, there are only two places where real ''joints'' showing a great deal of rotational movement of elements can be identified (Fig. 1A). These two areas, the quadrate articulation and the cranial articulation, are described in detail below.

Miles (1969) described the feeding mecha-

nism of the arthrodire placoderm *Coccosteus cuspidatus* as involving a simultaneous lifting of the cranium and lowering of the mandible. The lower jaw is composed of an ossified inferognathal element surrounded by Meckel's cartilage. Part of this cartilage forms the articular, with a dorsally oriented fossa. A condyle fused to the inside of the cheek plate fits into this fossa to form the quadrate joint. This joint restricts the mandible to dorsoventral movement (Miles 1969). The jaw suspension in arthrodires is considered to be autostylic, meaning that the jaw is suspended directly from skull elements without any involvement of the hyomandibula. The palatoquadrate of *Dunkleosteus* was fused to the suborbital cheek plate and reduced to only an anterior autopalatine element and the posterior quadrate element, rendering it essentially immobile. The condition of the hyomandibular element is unknown. Although it is still unclear what the primitive placoderm condition is, the hyomandibula likely has no role in jaw depression in arthrodires (Miles 1969; Johanson 2003; Anderson 2008).

Arthrodires (including *Dunkleosteus*) likely utilized cranial elevation during feeding to increase gape (Fig. 1D) (Miles 1969). A pair of endoskeletal and dermal cervical joints facilitates this movement. The endoskeletal joints lie between the endocranium and fused synarcual elements of the vertebrate. The dermal joints (called ''cranial joints'' in this paper) consist of transversally elongate condyles on the anterior dorsolateral plates of the thoracic armor, which fit into a set of posterior-facing fossa on the paranuchal plates of the skull. The orientation of these joints restricts movement to a purely dorsoventral rotation of the skull (Miles 1969).

Four hypothesized muscle blocks drive the movement of these elements in *Coccosteus*, and likely other arthrodires including *Dunkleosteus* (Fig. 1C) (Miles and Westoll 1968). The cranium is raised by the anteriormost portions of the epaxial muscles, which originate on the dorsal plates of the thoracic armor and insert onto the dorsal face of the occipital region of the brain case, as in recent fishes (Miles 1969). The skull is lowered by a series of muscles that originate on the upper postbranchial laminae of the anterior dorsolateral plates of the thoracic armor and insert onto large embayments on the medial surface of the paranuchal plates of the skull (Miles 1969). The jaw is depressed via hypobranchial muscles that run between the ventral portion of the thoracic armor and the anterior portion of the Meckel's cartilage at the symphysis of the jaws. This muscle is likely homologous to the coracomandibular muscle of modern chondrichthyans (Johanson 2003; Anderson 2008). The adductor muscle originates from the thickened lateral part of the visceral surface of the skull roof and part of the omega-shaped palatoquadrate and inserts onto the lateral surface of the inferognathal element (Miles 1969). Possible mandibulohyoid ligament attachment surfaces are most likely not functional (Johanson 2003), and there is no evidence for a hyoid-mandible coupling controlling jaw depression in placoderms as it does in teleosts (Lauder 1980).

Dunkleosteus exhibits the same basic morphology that Miles (1969) described in *Coccosteus* (Fig. 1A,C). In *Dunkleosteus*, the cranial and quadrate joints create a potential four-bar linkage in the skull and thoracic armor (Fig. 1D). The thoracic armor remains stationary relative to the rest of the system. The cranial armor acts as one of the rotation elements, rotating around the cranio-thoracic joint. The free element is the inferognathal (lower jaw) itself and the fourth element is the hypobranchial muscle, which tethers the inferognathal to the thoracic armor (as reconstructed by Miles [1969]). As the cranial armor is rotated dorsally, the quadrate joint is pulled forward and the inferognathal is forced to drop due to its connection to the thoracic armor (Fig. 1D). This hypothesis of cranial lift driving jaw depression through a series of links is modeled as a four-bar linkage mechanism unlike those seen in modern teleosts, which use jaw depression to drive premaxillary protrusion (Westneat 1990; Anderson and Westneat 2007).

The Computer Model

The placoderm feeding mechanism was modeled as a four-bar linkage, in a manner similar to previous dynamic linkage analyses of fish jaws (Westneat 1990, 2003; Anderson

and Westneat 2007). A computer model was developed using Metrowerks CodeWarrior Pascal (application available from M. Westneat). The model accepts sets of 33 Cartesian coordinates in lateral view that quantify placoderm skull morphometrics. The computer model (PlacoderModel 2.0) allows simulation of epaxial and jaw depressor muscle contraction, and predicts cranial elevation, jaw rotation, gape, and other kinematic variables.

The software program NIH Image (with Jeff Walker's Quick Image add-on; http://www.usm.maine.edu/~walker/software.html) was used to determine the coordinates of landmarks, as well as scale. The landmarks represent the four-bar linkage model, muscle reconstructions, and general shape as shown in Figure 1B. Landmarks 5, 16, 22, and 26 delimit the points of rotation for the four-bar linkage. Landmarks 21 and 27 represent the extent of the epaxial muscles used to lift the cranium. Miles (1969) concluded that the epaxials involved in cranial elevation were only the very anteriormost blocks. Landmarks 15 and 32 indicate the ends of the cranial depressor muscle based on the ventral morphology of the skull roof. Landmarks 5 and 26 indicate the attachments of the jaw depressor muscle. Most *Dunkleosteus* specimens lack a preserved palatoquadrate cartilage, so it is not possible to determine exactly where the adductor would originate on the suborbital plate. We estimate that the adductor originated on the cranial roof, behind the postorbital process and lateral to the endocranium (Long 1995). This origin was chosen because the omega shape of the placoderm palatoquadrate indicates that this cartilage abutted against the cranial roof. Therefore, the adductor muscles attaching to the palatoquadrate were separated from the skull roof only by the cartilage itself (Long 1995). This makes the cranial roof a good upper estimate for the length of the adductor muscles. However, it is still not clear where along this edge the palatoquadrate lies, so we selected two points (12–13) to give a range for the muscle. Landmarks 11 and 20 give the extremes of a range of possible sites of adductor insertions along the inferognathal. The rest of the landmarks describe the general shape of the various elements.

We estimated muscle volume for the four muscle blocks for one of the specimens (CMNH5768). Polyurethane foam blocks were carved to fit into the space available for the four muscles of interest (adductor mandibulae, jaw depressor, epaxials, and cranial depressor). We then wrapped the muscles in shrink-wrap and submerged them to obtain the volume via displacement. Calculated geometric volumes verified the submersion estimates. Further data on these muscle reconstructions in *Dunkleosteus* could affect these assumptions and alter the resulting bite force estimates reported below. Assuming a constant cross-sectional area for the muscle, the volume value divided by the length of the muscle equals cross-sectional area. For initial muscle simulations, we assumed a muscle contraction speed of 5 muscle lengths/s (similar to modern marlin). Maximal muscle stress was varied from 150 to 300 kPa, the range found in modern vertebrate muscle (Bone et al. 1986; Curtin and Woledge 1988; Medler 2002). It is not possible to know the exact muscle architecture of a fossil fish, so we assumed parallel-fibered muscles because many cranial muscles in fishes exhibit this arrangement.

Biomechanical Simulations of Placoderm Feeding

Mechanical advantage (MA) is the ratio of the inlever to the outlever and is a measure of force transfer by a lever mechanism such as the lower jaw. The inlever is the distance from muscle insertion on the jaw (landmarks 10 or 17) to the jaw joint (landmark 16) (Figs. 1B, 2), and the outlever is the distance from jaw joint to the jaw tip (landmark 4) or back dentition (landmark 9) (Westneat 2003). Effective mechanical advantage (EMA) is the MA multiplied by the sine of the angle of insertion of the muscle. In a four-bar linkage system, the ratio of the output rotation to input rotation is commonly called the kinematic transmission coefficient or KT. It is a measure of the motion transferred across the linkage. The reciprocal of this ratio is the force transmission, and it measures the force transfer across the linkage, analogous to mechanical advantage in levers. Both levers and linkage systems show a tradeoff between force and motion transfer in

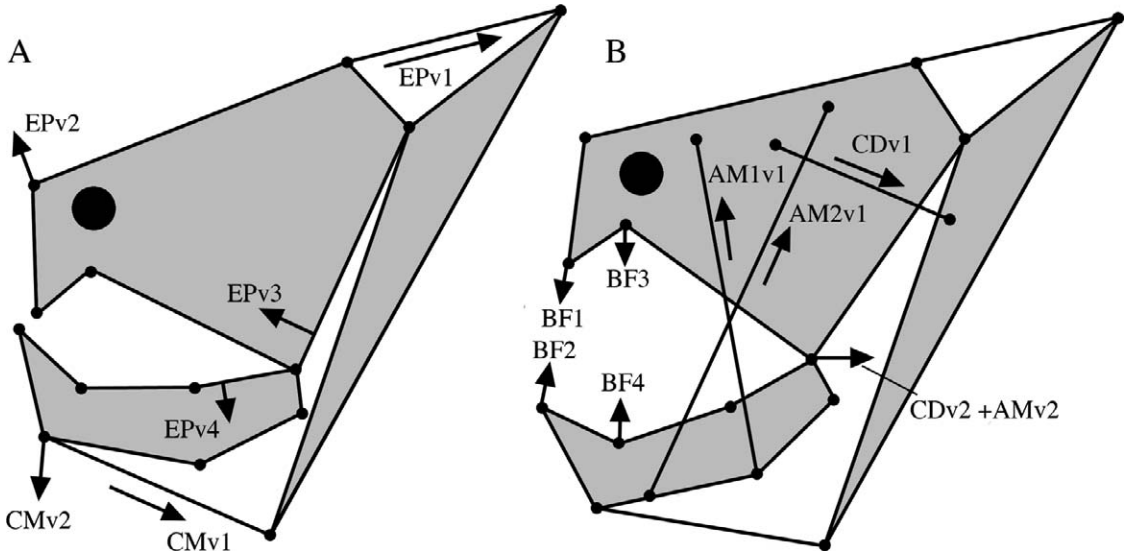

FIGURE 2. Vector diagrams of the biomechanics of feeding in *Dunkleosteus terrelli* illustrating jaw opening (A) and jaw closing (B). A, During jaw opening, the muscle input force vectors (epaxialis vector 1- EPv1) and coracomandibularis vector 1 (CMv1) cause cranial elevation (EPv2) and lower jaw depression (EPv3–4 via the linkage). B, Jaw-closing mechanics are driven by force vectors of the cranial depressor (CDv1) and the adductor mandibulae, reconstructed in two configurations (AM1v1, AM2v1). Bite force is exerted by both lever and linkage force vectors if a prey item is caught between the anterior fangs (BF1 and BF2) or between the rear dental blades (BF3 and BF4). (Modified from Anderson and Westneat 2007.)

which an increase in mechanical advantage comes at a cost to velocity transmission, and vice versa.

Jaw Opening.—Cranial elevation and lower jaw depression were computed by simulating contraction of the jaw opening muscles, including the epaxial (EP) muscles, which originate on the thoracic shield and insert on the rear of the skull, and coracomandibularis (CM) muscle, which originates on the scapulocoracoid and inserts on the lower jaw. The EP muscle rotates the skull dorsally around the cranio-thoracic joint between the thoracic shield and the posterior skull (Fig. 2, EPv2), and rotates the four-bar linkage open near the jaw joint (Fig. 2, Epv3) whereas the CM muscle rotates the mandible ventrally. Because of tension in the CM, EP force is transmitted all the way to the jaw (Fig. 2, Epv4) to contribute to mandibular rotation. The jaws open in a readily computable pattern due to the mechanics of the four-bar linkage, for which the thoracic shield is the fixed link, the skull is the input link, the CM muscle is a second anchored input link, and the lower jaw is the output link whose motion is determined by skull motion and CM length (Fig. 2).

Jaw Closing.—The cranial depressor and adductor mandibulae muscles were simulated to lower the skull and close the jaws, starting from maximal gape position (set at 45° gape angle in our simulations). For each specimen, two adductor orientations were examined: A1 (muscle originates at landmark 12, the anteriormost point right behind the eye, and inserts at the posteriormost point along the lower jaw, landmark 20); A2 (muscle originates at the posteriormost point along the skull roof, landmark 13, and inserts on the lower jaw at the anterior most point behind the dentition, landmark 11) (Fig. 1C). Jaw closing is also governed by the mechanics of the four-bar linkage, assuming that the CM muscle is relaxing but remains in tension as the linkage returns to its rest position. Jaw-closing muscles were simulated to shorten through a series of iterations until the skull and jaws returned to their closed positions.

Feeding Kinematics and Forces.—Dynamic contractions of the jaw-opening muscles were

simulated in increments of 0.5% resting length up to approximately 10% shortening, then the pattern was reversed, driving the system with the cranial depressor and jaw closers. These simulations focused on linkage motion, assuming that the skull closes without encountering a prey item. The simulation steps and variables calculated were (1) EP and CM contraction in increments of 0.5% until 45° gape angle achieved; (2) skull rotation angle due to EP contraction (Fig. 1C); (3) lower jaw rotation angle due to linkage action and CM contraction (Fig. 1C); (4) kinematic transmission coefficient (KT), a heuristic measure of linkage speed that equals output rotation of the jaw divided by input rotation of the skull; (5) gape distance and gape angle; (6) closing-muscle stretch restricted to physiologically feasible muscle percentages of 10–20%, (7) jaw-closing motions driven by the jaw closing muscles, including gape, gape angle, linkage rotations, and KT in computations similar to those for jaw opening.

Bite Force.—We examined each of the positions of the closing jaws for the potential to exert bite force on a prey item, if a prey item were encountered between the jaws at that position. The CD rotates the skull downward and pushes the jaw joint rearward (Fig. 2, CDv2). The AM force vector rotates the jaw around its joint with the skull and forces the jaw joint rearward (Fig. 2, AM2v2). Thus, downward force from the upper jaw (Fig. 2, BF1 and BF3) is composed of CD output force exerted by the large skull lever and by AM2v2 force, which is transmitted to the skull by the four-bar linkage. Lower jaw bite force (Fig. 2, BF2 and BF4) is generated solely by the powerful lever advantage of the AM muscles. We used the physiological cross-sectional area of the cranial depressor and jaw adductors (A2 reconstruction) to calculate their force potential during closing and computed the fraction of that force that was effectively transmitted through the four-bar linkage as bite force. The A2 reconstruction has a higher mechanical advantage than the A1, and will give us an upper limit to bite forces. These computations, performed dynamically at each iteration of the model through the closing cycle, involved resolving the force balance of each muscle at each joint and calculating mechanical advantage, torque, linkage force transmission, and final bite force. The variables calculated were (1) mechanical advantage (MA), the ratio of inlever to outlever of the jaw; (2) effective mechanical advantage (EMA), mechanical advantage multiplied by the sine of the angle of muscle insertion; (3) torque and output force of CD and AM muscles at the jaw tips and at the posterior point of the inferognathal blade; and (4) bite force, the total resultant bite force vectors for both muscles in both bite positions, multiplied by 2.0, assuming bilateral contraction on both sides of the skull.

Bite force estimates for the smaller skulls were based on the computations for the large skull and its direct muscle volume measurements. We assumed that the muscle volumes of the smaller specimens had the same proportion to total skull size and volume as the single measured specimen, and we used those volume estimates to compute cross-sectional area and bite force.

Effects of Skull Mass.—The computational model assumes that the muscles are capable of transmitting their forces and resulting motions through the linkage joints with no friction loss and are capable of lifting the skull with no loss of velocity or force potential due to the mass of the skull or the density of water. These assumptions result in an overestimate of rotation speeds for the large skulls modeled here, so we assessed the effects of skull mass and entrained water mass during rapid head lifting by computing the cranial center of mass and the rate of acceleration that the epaxial muscle force would provide for rotating the cranial mass around the cranio-thoracic joint. We calculated this for the skull alone and for the skull plus the sphere of water entrained in the ''added mass'' due to inertial drag of the surrounding water.

Results

The biomechanical feeding model based on a novel four-bar linkage mechanism in the skull and thoracic armor of *Dunkleosteus terrelli* provided a wide range of kinematic parameters and bite force estimates for the feeding strike of one of the largest aquatic predators of the Devonian (Fig. 3). The primary re-

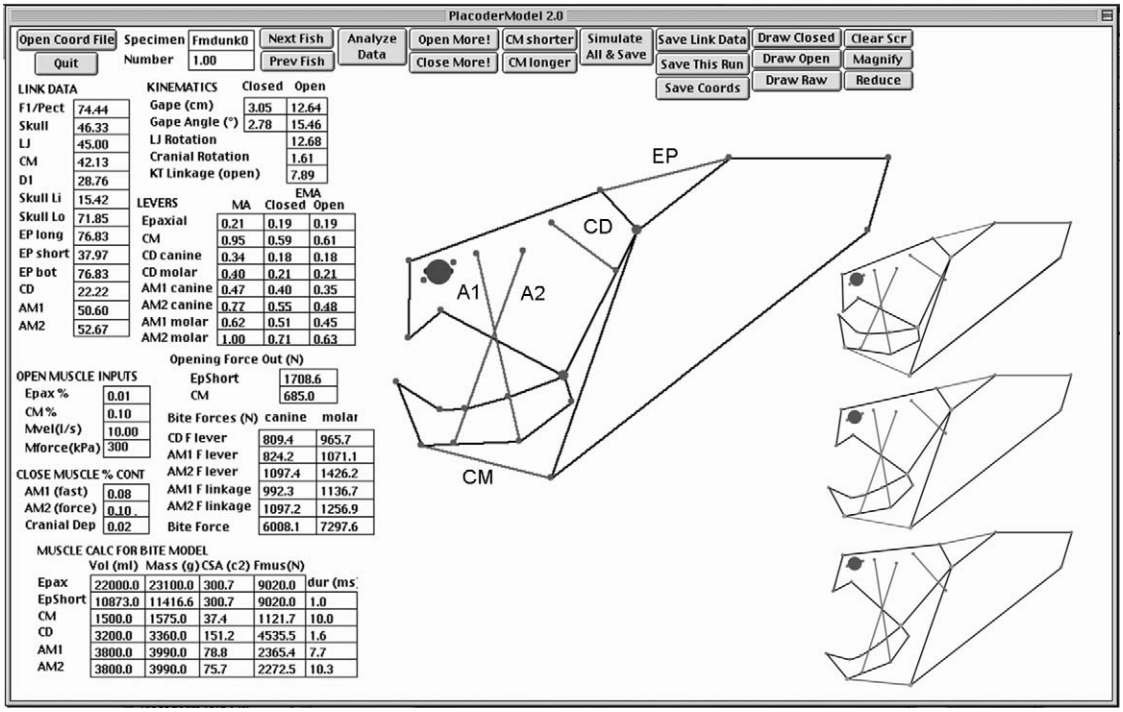

FIGURE 3. Screen shot of PlacoderModel 2.0. The interface allows the landmark data from specimens to be loaded and analyzed. The line drawing is a rough shape of the skull, for visualization purposes, and the boxes on the left show the entered measurements and resulting metrics based on the epaxial and/or jaw depressor contractions entered. EP, epaxial muscle; CD, cranial depressor muscle; A1, adductor reconstruction 1; A2, adductor reconstruction 2; CM, coracomandibular muscle. The simulated positions of kinetic skeletal elements are shown as the three smaller skull schematics.

sults of this study are the following. First, the novel four-bar linkage system appears to be a realistic hypothesis for the jaw and cranial movements in *Dunkleosteus terrelli* during feeding, and the reconstructed muscles undergo realistic amounts of strain during simulated gape cycles. Second, the model suggests that *Dunkleosteus* could expand its gape very rapidly, with higher KT (2.0–4.0) values than the oral linkages measured in modern fish. Finally, bite force estimations (~6000 N) are among the highest of any living or fossil fish group measured. These high bite forces are due not only to the overall size of the muscles involved, but also to the linkage system, which adds around 1000 N to the overall bite force. The estimated maximum stress assumed for cranial muscles in *Dunkleosteus* has a profound effect on bite force as well, providing a set of confidence limits on bite forces in this species.

Feeding Kinematics in *Dunkleosteus*

During the jaw-opening cycle (Figs. 3, 4, from specimen CM5768), the epaxials and jaw depressor muscles contract at the same rate until a gape of ~45° is achieved. Rotating the skull dorsally causes the quadrate articulation to swing up and forward. The jaw depressor muscle acts as a tether and forces the lower jaw to swing downward, opening the mouth. Contraction on the jaw depressor enhances this movement. Figure 4A–D shows the pattern of skull rotation, jaw rotation, and gape angle for all five skulls. Table 1 shows the percent epaxial and jaw depressor (CM) contractions when peak gape is attained.

The maximum possible gape (45°) is constrained by the placement of the adductor muscles. As the jaws open, the lines of action of the adductors move posteriorly relative to the lower jaw (Fig. 3). At a gape of 45°, the muscles press up against the quadrate artic-

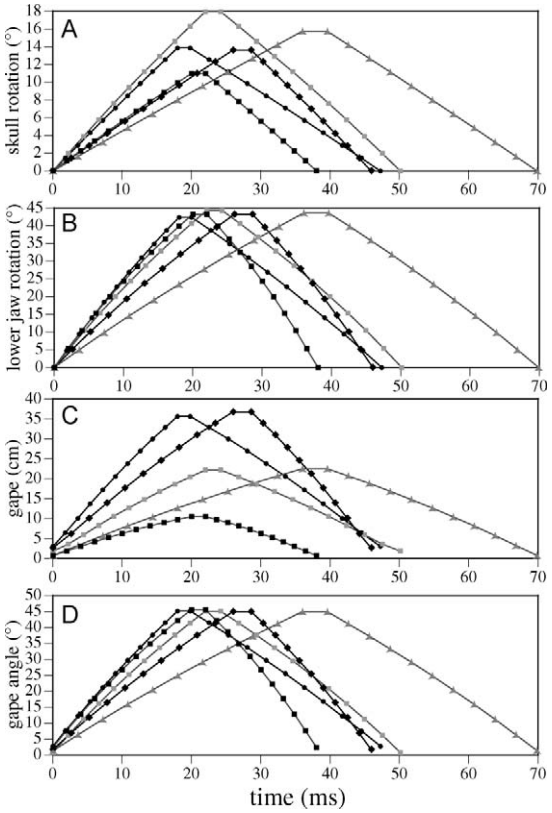

FIGURE 4. Simulated kinematics of skull kinesis in five specimens of *Dunkleosteus terrelli* generated using a biomechanical model of four-bar linkage motion, including skull rotation (A), mandibular rotation (B), gape distance (C), and gape angle during the feeding cycle (D). These motions are perfectly reversed in angle and position during closing, but the timing of opening and closing may differ because contraction duration of opener and closer muscles may vary.

ulation, preventing further opening. When the opening muscles (epaxial and CM) are contracted PlacoderModel 2.0 measures the resulting positive strain on the cranial depressor and adductor muscles as they are stretched. This is equivalent to the contraction necessary for the depressor and adductors to return the cranium and jaws to their initial positions. For each specimen both the A1 and A2 adductor orientations were examined (A1: landmark 12 to landmark 20; A2: landmark 13 to landmark 11). Both reconstructions show strain values of 10–30% for a maximum gape angle of 45° (Table 1).

TABLE 2. Static mechanical advantages for all five specimens. Specimens are ordered from largest to smallest. Abbreviations: CD, cranial depression; CM, coracomandibular; A1, closing mechanical advantage based on the anteriormost adductor insertion; A2, closing mechanical advantage based on the posteriormost adduction insertion.

Specimen	Epaxial	CD	CM	A2	A1
CM5768	0.21	0.34	0.95	0.77	0.47
CM7054	0.22	0.29	0.81	0.54	0.31
CM6090	0.26	0.32	1	0.79	0.58
CM7424	0.18	0.27	0.93	0.64	0.37
CM6194	0.19	0.31	0.89	0.59	0.3
Mean	0.21	0.31	0.92	0.67	0.41
Coef. var.	0.147	0.088	0.078	0.165	0.292

Mechanical Advantage, Opening Speed, and Bite Force

PlacoderModel 2.0 computes several mechanical metrics including static mechanical advantages for all of the muscles involved (Table 2). Cranial elevation and depression MA use the distance from the cranio-thoracic joint (landmark 22) to the front of the upper dentition (landmark 3) as an outlever and the lengths from the cranio-thoracic joint to the epaxial (landmark 21) and cranial depressor (landmark 15) muscle origins respectively as inlevers (Fig. 1B). The A1 and A2 jaw MAs refer to the two possible adductor insertions on

TABLE 1. Muscle contraction and strain percentages in five *Dunkleosteus* specimens at a gape angle of 45° (peak gape). Specimens are ordered from largest to smallest. Abbreviations: CM, Coracomandibularis (jaw depressor muscle); CD, cranial depressor muscle; A1, first adductor muscle (speed insertion); A2, second adductor muscle (force insertion); Coef. var., coefficient of variation (the variance of the data), scaled to the average.

Specimen	Epaxial	CM	CD	A1	A2	Skull length (cm)
CM5768	9%	11%	14%	21%	29%	72
CM7054	13%	14%	9%	10%	19%	56
CM 6090	11%	13%	13%	12%	11%	46
CM7424	18%	19%	15%	12%	14%	41
CM6194	10%	10%	8%	11%	20%	25
Mean	12%	13%	12%	13%	19%	
Coef. var.	0.292	0.262	0.264	0.336	0.37	

TABLE 3. Effective mechanical advantages and kinematic transfer coefficients (KT) when jaws are at a 45° gape angle and closed. Specimens are ordered from largest to smallest. Abbreviations: CD, cranial depression; CM, coracomandibular; A1A, A1 muscle, outlever measured to anterior fang; A1P, A1 muscle, outlever measured to posterior blade point; A2A, A2 muscle, outlever measured to anterior fang; A2P, A2 muscle, outlever measured to posterior blade point.

Specimen	Position	Epaxial	CD	CM	A1A	A1P	A2A	A2P	KT
CM5768	Open	0.19	0.18	0.59	0.396	0.515	0.548	0.712	2.76
	Closed	0.2	0.17	0.71	0.213	0.277	0.31	0.403	3.3
CM7054	Open	0.16	0.11	0.48	0.214	0.362	0.345	0.583	2.79
	Closed	0.18	0.10	0.63	0.059	0.1	0.143	0.241	3.58
CM6090	Open	0.16	0.12	0.77	0.306	0.414	0.322	0.437	2.25
	Closed	0.2	0.12	0.98	0.06	0.081	0.046	0.062	2.73
CM7424	Open	0.12	0.14	0.64	0.217	0.322	0.274	0.407	2.47
	Closed	0.13	0.13	0.8	0.051	0.075	0.079	0.118	3.07
CM6194	Open	0.13	0.13	0.35	0.21	0.36	0.375	0.643	3.2
	Closed	0.15	0.12	0.44	0.064	0.11	0.164	0.28	4.64
Mean	Open	0.15	0.14	0.526	0.269	0.395	0.373	0.556	2.69
	Closed	0.172	0.128	0.712	0.089	0.129	0.148	0.221	3.46
Coef. var.	Open	0.183	0.199	0.335	0.304	0.19	0.281	0.236	0.133
	Closed	0.181	0.202	0.281	0.775	0.654	0.688	0.611	0.21

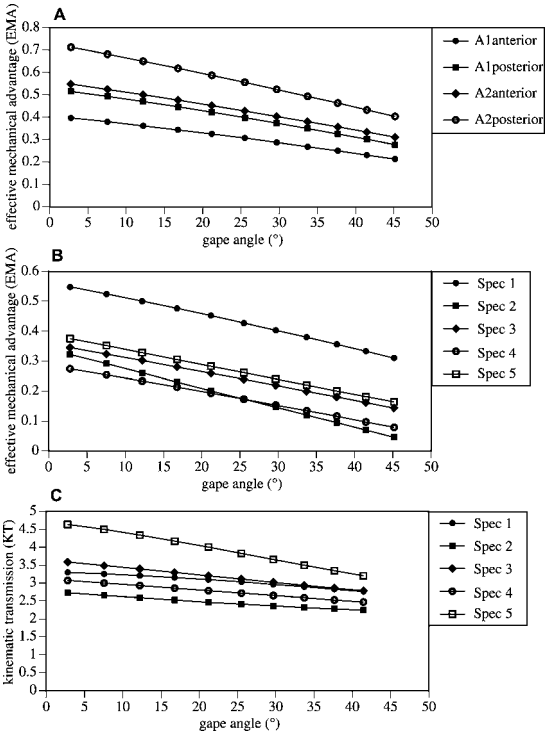

FIGURE 5. EMA and KT over gape angle in *Dunkleosteus*. A, EMA values for four different combinations of adductor reconstruction and placement along dentition in CM5768. B, EMA of adductor reconstruction A2 as the inlever and the anterior tip of the dentition as the outlever (A2anterior) in all five *Dunkleosteus* specimens. C, KT values over gape angle for all five *Dunkleosteus* specimens.

the lower jaw (landmarks 11 and 20). The cranial depressor muscle shows a range of MA values from 0.27 to 0.34 and the adductor muscles show ranges of 0.54–0.79 for the anterior insertion and 0.30–0.58 for the posterior insertion (Table 2). These are static mechanical advantages as measured directly from the jaw elements; they do not recognize changing geometry during the feeding cycle.

The effective mechanical advantages (EMA) and kinematic transmissions (KT) for each individual (Table 3) vary depending on the muscle insertion angle, which changes with gape angle. The four jaw EMAs are based on the two possible adductor muscle placements (A1, A2) with outlevers measured to either the anterior fang (A) or the posterior most point of the bladed dentition (P). Because the EMA is influenced by the angle of force applied to the beam, in this case the angle of muscle insertion, these values will change through the feeding cycle (Fig. 5). The cranial depressor muscle shows EMA values of 0.13–0.2 when the jaws are closed and 0.12–0.19 at peak gape. The highest adductor EMAs occur when using the A2P configuration (0.062–0.43 when jaws are closed, 0.407–0.712 at peak gape) and the lowest EMA values occur using the A1A configuration (0.051–0.213 when closed, 0.21–0.396 at peak gape; see Table 3 for full results). Neither the cranial elevator nor depressor EMA changes much during the feeding cycle.

TABLE 4. Bite force estimates for specimen CM5768. Maximum muscle stress set at 289 kPa. Abbreviations as in Table 3.

	When closed	At gape of 45°
A1A	5265 N	2766 N
A1P	6371 N	3380 N
A2A	6170 N	3133 N
A2P	7495 N	3858 N

However, jaw EMA decreases as the mouth opens and the muscle angle becomes more and more acute (Fig. 5B). In all specimens the highest EMA is just as the mouth is closed and the lowest is at maximum gape. KT also decreases as gape angle increases, illustrated in Figure 5C, which shows the change in KT across gape angle in the five specimens, ranging from 2.73 to 4.64 when jaws are closed and from 2.25 to 3.2 at peak gape (Table 3).

The bite-force estimate for CM5768 (Table 4) is based on three different sources of force during closing: (1) Force produced by the cranial depressor muscle (Fig. 2, CDv1). The force generated by the CD muscle is transferred through the skull and results in peak forces of 800 N on the anterior fang and close to 1000 N on the back of the jaw (Fig. 6). (2) Adductor force through the jaw levers. As with the EMA measures, only two of the adductor reconstructions were considered (Fig. 2, AM1v1 and AM2v1). The force produced by these muscles is transferred through the jaw lever and results in peak forces from 800 N using the A1 reconstruction on the front of the jaw to 1600 N using the A2 reconstruction on the back of the jaw (Fig. 6). (3) Adductor (and CD) forces acting through the linkage system (Fig. 2, CDv2 + AM2v2). The muscles acting to lower the skull and raise the lower jaw also act to pull the quadrate joint backward and transfer force through the linkage system (Fig. 2). This action adds 80–1000 N of force at closed gape (Fig. 6).

The numbers above are based on forces at a closed gape (maximal bite force); however, each position of the closing jaws was examined for the potential to exert bite force on a prey item, if a prey item were encountered between the jaws at that position. The highest overall peak force (7495 N) was obtained

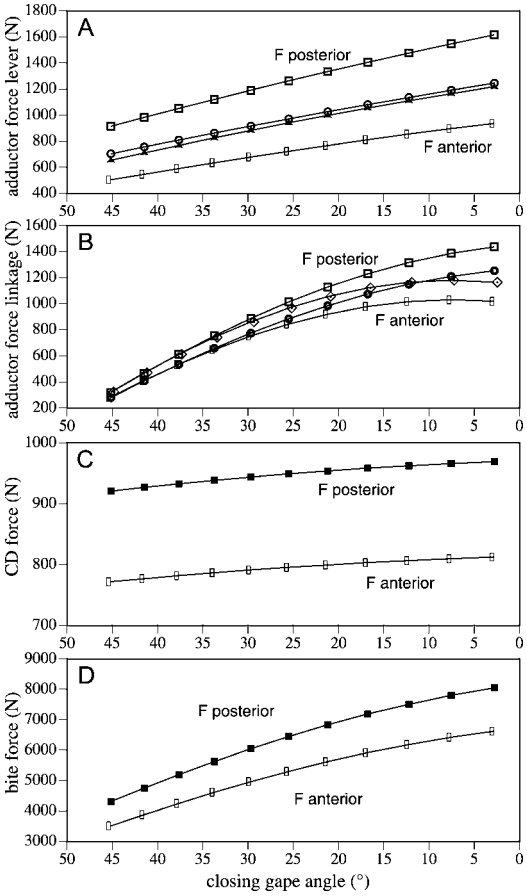

FIGURE 6. Forces produced during jaw closing for the largest *Dunkleosteus* specimen (CM5768). Symbols represent different reconstructions. Squares: bite fore measured from the back of the dentition. Circles: bite force measured from the front of the dentition. Open symbols: A2 adductor reconstruction. Closed symbols: A1 adductor reconstruction. A, Resulting force transferred by the adductor muscles through the jaw lever. B, Forces produced by the adductor muscles transferred through the linkage system. C, Resulting forces from the cranial depressor muscles transferred through the skull lever. D, Overall resultant bite forces estimated by summing all the individual bite force components.

when the jaws were fully closed and these force estimates are among the highest reported for any modern sharks or fish (Wroe et al. 2008; see Huber et al. 2005, for a comprehensive list of measured taxa). They are also higher than any reported for terrestrial carnivores except for some alligators (13172 N [Erickson et al. 2003]). Bite force varies both with skull size and with the underlying maximum muscle stress used for the analysis (Fig. 7).

For CM5768, it was also possible, using the

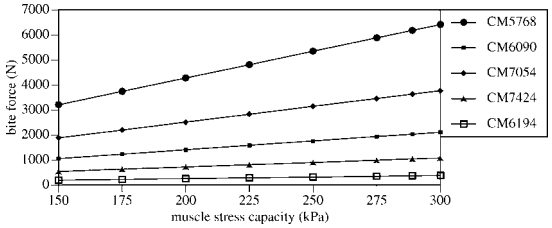

FIGURE 7. Maximum muscle stress versus bite force for the A2 reconstruction at closed gape for all five skulls. Muscle volume was measured directly from foam models for CM5768. Muscle estimates for the other four skulls are based on a scaling factor of CM5768. The size of the skull affects not only the magnitude of bite force, but also the range of bite forces based on varying maximum stress estimates.

muscle volume estimates, to calculate the time necessary to achieve peak gape. However, to get at the realistic speed for gape expansion in *Dunkleosteus* we had to account for the mass of the skull and entrained water during opening. The skull of CM5768 was 72 cm long and approximately 36 cm tall and wide, for a total volume of 93,312 cubic centimeters, or about 98 kg, assuming the density of seawater. If the volume of entrained seawater around the skull during feeding were a sphere of 72 cm diameter, the result would be a mass (including skull plus water) of about twice that, or 205 kg. The force of the epaxial muscle was 6013 N, transmitted through a lever mechanism with a mechanical advantage of 0.42 to the center of mass of the skull. Assuming that this force was constant (an acknowledged simplification of muscle kinetics), the effective output force available to lift the skull at the CM was thus 2525 N (torque = 909 N·m). Dorsal acceleration of the skull, averaged over the 15° rotation of the cranium, equals 25.8 $m \cdot^{-2}$ for the skull alone and 12.3 $m \cdot^{-2}$ for the skull plus entrained sphere of water. Total skull rotation was 15°, displacing the center of mass about 10 cm. When neither skull mass nor entrained water was accounted for, skull lifting took only 18 ms. Under the ''skull only'' simulation, lifting the skull would require 45 ms, whereas under the ''skull + water sphere'' assumption, less than 60 ms would be required.

Discussion

The novel four-bar linkage model of the skull and armor designed to predict cranial and jaw movements is a realistic and informative model for prey capture ability and function in the arthrodire placoderm *Dunkleosteus terrelli*. The model we developed here offers new insights into the feeding behavior of this fossil group, with four main points. (1) The maximum gape attained by *Dunkleosteus* is restricted by the strain and position of the adductor muscles rather than the geometry of the nuchal gap. The large nuchal gap in *Dunkleosteus* has other mechanical consequences related to the linkage system. (2) *Dunkleosteus* appears to have had rapid gape expansion and possibly utilized suction forces during prey capture. (3) Estimated bite force capability is among the most powerful bites measured in either living or fossil animals. (4) The metrics produced by the model support the idea that *Dunkleosteus* was an apex predator of the Late Devonian, well adapted to capturing and processing the prey species found in its habitat.

The Novel Four-bar Linkage of *Dunkleosteus terrelli*

The computer model and simulations of the skull and thoracic armor of *Dunkleosteus terrelli* suggest that a four-bar linkage mechanism is a valid hypothesis for the dynamics of feeding in this group. Physiologically typical epaxial and CM contractions produced realistic values of cranial and jaw rotation, comparable to those in modern fishes. Cranial fast muscles in modern fishes typically contract 5–20% during a feeding cycle (Bone et al. 1986; Curtin and Woledge 1988; Medler 2002). The strains placed on the adductor muscles during jaw opening fall within this range for four of the skulls tested, the exception being specimen CM5768, whose muscle strain percentages for the adductor muscles for a gape of 45° are well above those for the other specimens. It is not clear whether this discrepancy is due to the larger size of this specimen (skull length is 16 cm longer than the next largest, CM7054) or some other aspect of the skull shape. In effect, it possibly reduces the peak gape capabilities of this large specimen, but further speculation must wait for additional taxa to be examined.

The combination of muscle strain values

and adductor muscle position allows a maximum gape angle to be established for *Dunkleosteus*. At a gape angle of 45°, the adductor muscles fall within the typical 5–20% strain for vertebrate muscle. If the gape is increased beyond this point, the adductors begin to show unrealistic strain values and shift to a position behind the quadrate joint (Fig. 3), which is a physical impossibility for continued function. It has long been assumed that the nuchal gap, located dorsally between the nuchal plate on the skull and the median dorsal plate of the thoracic armor (Fig. 1A), indicates the total amount of cranial rotation possible in arthrodires. Miles (1969) reinforced this hypothesis in his study of coccosteids, which showed that the nuchal gap must ultimately limit arthrodire gape. However, the model presented here shows that peak gape is achieved well before the nuchal gap in *Dunkleosteus* is closed (Fig. 3).

The larger nuchal gap in *Dunkleosteus* affected cranial lift in another way. The nuchal gap of *Coccosteus* is much smaller relative to body size and may be the limiting factor in that taxon. Increasing the size of the gap in *Dunkleosteus* increases the length of the epaxial muscle used to lift the cranium and the lever arm between the cranial joint and the point of attachment for the epaxials on the skull roof. Lengthening the muscle increases the contraction length, whereas lengthening the lever arm results in higher mechanical advantage during opening. A higher mechanical advantage would allow greater force during cranial lift, important when lifting a large cranial shield like that in *Dunkleosteus*.

The current four-bar linkage model does not take the hyoid element of *Dunkleosteus* into account. Most modern osteichthyans initiate gape expansion during feeding by depressing the hyoid and lower jaws together through a hyomandibular ligament (Lauder 1980). Modern chondrichthyans do not exhibit coupled depression. Two muscles, the coracohyoideus and coracomandibularis, both originate on the pectoral girdle and depress the hyoid and mandible separately (Wilga et al. 2000). Pieces of the hyoid arch have not been definitively identified in placoderms though possible hyoid fragments have been found out of life position (Long 1997). Possible attachment surfaces for a mandibulohyoid ligament on the articular cartilage have been identified in a few placoderms (Johanson 2003). Although a ligament may be present, it is not necessarily functional in the way seen in teleosts, as certain chondrichthyans with uncoupled jaw action also have this ligamentous connection (Allis 1923). If additional anatomical details on the *Dunkleosteus* hyoid come to light, it would be an interesting additional musculoskeletal element for biomechanical modeling.

Speed and Force of *Dunkleosteus* Feeding

Miles (1969) asserted that *Dunkleosteus* had a slow, powerful bite. However, the results of the skull model developed here indicate that *Dunkleosteus* had fairly rapid jaw rotation during the opening phase, with gape angle increasing at more than 2° per millisecond in most individuals. The range of KT values during opening between the five specimens ranges from 2.0 to 4.0, considerably higher than the KT range of 0.5–1.52 for 300 labrid fishes with diverse prey preferences (Wainwright et al. 2004) Most teleosts have both an oral jaw linkage and a hyoid linkage that controls depression of the hyoid bar and suction feeding (Westneat 1990). The range found by Wainwright et al. (2004) for the hyoid linkage was 0.07–4.7 among modern labrids. *Dunkleosteus* KT values fall in the mid to high area of this range. *Dunkleosteus* had a rapid opening mechanism, well above the range of modern oral linkages and comparable to the upper range for many hyoid linkages.

It is possible that *Dunkleosteus* produced suction forces for feeding during jaw opening. The production of suction pressure during feeding in modern fishes requires both rapid gape expansion and a large increase in the volume of the throat and mouth cavities (Ferry-Graham and Lauder 2001; Sanford and Wainwright 2002; Carroll et al. 2004; see Westneat 2006 for a review). Estimates based on muscle reconstructions in the largest specimen (CM5678) and assumed muscle speeds of 5 lengths/s give value for gape expansion of ~60 ms, which closely matches the opening durations for modern suction feeding nurse sharks (Motta et al. 2002). This estimate ac-

counts for both skull mass and entrained water volume during opening as well. Further evidence for suction comes from the increase in oral volume seen in the model during gape expansion (Fig. 3). This expansion is entirely in the dorsoventral dimension, but several modern suction feeders are able to generate sufficient volume changes with solely dorsoventral movement as well (Van Wassenbergh et al. 2004). Although less complex than the suction mechanisms of modern fishes, a large and rapid increase in oral volume during gape expansion would lead to a large pressure gradient, creating a suction force in front of the opening. The utility of this suction force is unclear, because it is unknown how big the oral opening would have been in *Dunkleosteus*. Fossil remains indicate a wide gape and open sides, which would reduce the flow velocities into the oral cavity. However, it is unknown if soft tissues were present, which would prevent leakage out of the ''cheeks.'' Alternatively, initial feeding may have involved a ram strategy, with intraoral suction used for continuing rearward prey transport in a manner similar to aquatic feeding in snapping turtles (Lauder and Prendergast 1992).

Dunkleosteus had one of the most powerful bites estimated in vertebrate history. The biomechanical source of high bite forces in *Dunkleosteus* is large adductor muscles with high cross-sectional area, the efficient force transmission characteristics of a four-bar linkage (Figure 2), and high mechanical advantage of the jaw-closing lever. The jaw-closing muscles (CD and AM2, Fig. 2) transmit their forces to the skull, the lower jaw, and the four-bar linkage to generate maximum bite forces of 6170 N on the anterior fang and 7495 N on the posterior part of the blade (Fig. 6). Simulation of an alternative muscle position (AM1, Fig. 2) resulted in slightly lower bite forces, from 5265 N anteriorly to 6371 N posteriorly. The high bite force values are partly due to extra force being transferred through the linkage system. One of the links in this system is the jaw depressor muscle, linking the lower jaw to the thoracic armor (Fig. 1). Because this is a muscle, it will act as a link only under tensile strain, not compressive strain. However, during jaw closing, if the lower jaw is lifted at a faster rate than the cranium is lowered, this muscle could remain in tension and pull the quadrate joint backward, the reverse of the motion seen during gape expansion. The use of the linkage system during closing adds up to 1000 N of force to the bite.

These calculations assume a maximal muscle stress of 289 kPa, equivalent to that in modern sharks. In a previous publication (Anderson and Westneat 2007) 200 kPa was used for maximum muscle stress, resulting in lower values. However, even for the lowest muscle stress tested (150 kPa), the resulting bite forces are 3202 N for A2 (Fig. 7) and 3890 N for A1. These values greatly exceed the bite forces for most other fish species that have been reported (Huber et al. 2005) and most modern mammalian predators, including the lion, black bear (Wroe et al. 2005), and spotted hyena (Binder and Van Valkenburgh 2000), this last having the highest bite force among carnivorous mammals, known to crack large bones with its jaws. The only higher bite forces are those calculated for large (+3000 kg) great white sharks (Wroe et al. 2008) and some alligators, and those estimated for dinosaurs (Erickson et al. 1996, 2003). Bite forces scale with size (Huber et al. 2005) and this is seen in the five *Dunkleosteus* skulls analyzed (Fig. 7). This scaling factor also helps explain the vast difference in magnitude between our estimated bite in *Dunkleosteus*, and the measured bite forces other fish. The largest fish with a bite force measurement in Huber et al. (2005) is *Carcharhinus limbatus* (blacktip shark), which measured 22 kg and has a bite force of 423 N (Weggelaar et al. 2004). The largest *Dunkleosteus* specimen we used is estimated to be 6 m long and 1000 kg. The bite force estimates for this largest skull fall above a recently compiled scaling trend of increasing bite force with body mass (Huber et al. 2005). However, when the 200 kPa muscle stress is used, the bite force values fit the trend closely (Anderson and Westneat 2007). Based on this scaling factor, estimated bite forces in *Carcharodon carcharias* (great white) exceed 9000 N for a shark over 3000 kg (Wroe et al. 2008). *Carcharodon megalodon* at 48,000–100,000 kg may have had a bite force exceeding a staggering 100,000 N (Wroe et al. 2008).

The bite force estimates reported here are based on specific muscle reconstructions for *Dunkleosteus*. The two alternative muscle reconstructions simulated here bracket the range of likely muscle configurations that are physically possible within the *Dunkleosteus* skull, with both origin and insertion modeled as anteriorly and posteriorly located. New anatomical work on *Dunkleosteus* and other arthrodires indicates that the fossa we used to estimate the size of the cranial depressor muscle may have housed more than just that muscle (R. Carr personal communication 2008). This would reduce the size of the CD muscle and lower our estimated bite force. One of the strengths of our model is its adaptability to new data such as this. If revisions to muscle volume or cross-sectional area are required, the new measurements can be entered into the model and a new set of bite force estimates can be calculated.

Prey Choice in *Dunkleosteus*

Our estimates of rapid expansion during jaw opening coupled with high bite forces during jaw closing indicate that *Dunkleosteus* was potentially using suction feeding for capturing evasive prey, as well as breaking through armor or bony materials once the prey was grasped in the jaws. The bladed dentition and fangs seen in *Dunkleosteus* and other arthrodire groups provided for extremely high local bite stress as the bite force was focused into a small area, the fang tip or blade edge. The focused high pressure likely enabled *Dunkleosteus* to puncture or cut through hard materials such as cuticle or dermal armor, thereby reducing large prey into smaller pieces.

Prior studies have suggested that placoderms with more blade-like dentition (such as *Dunkleosteus*) could take bites out of larger prey that are too big to swallow whole (Gross 1967; Miles 1969). The shape and form of dental elements are related to the mechanical properties of the food material being masticated, particularly to the energy necessary to propagate cracks and fragment the material (Lucas 2004). The bladed dentition of *Dunkleosteus* would be most useful for dealing with tough, extensible materials, such as the soft tissue of an animal (Lucas 2004). However, a recent study on the effects of bladed tooth shape on cutting ability has shown that certain bladed morphologies could be quite effective at slicing through more resilient materials such as cuticle (Anderson and LaBarbera 2008). Further, one of us (Anderson) has observed specimens of both *Dunkleosteus* (CM5302) and another related taxon, *Titanichthys* (CM9889) that show obvious damage due to puncturing by *Dunkleosteus* anterior ''fangs'' (G. Jackson personal communication 2005).

The Cleveland Shale is known primarily for its placoderms, but it also contains chondrichthyans (selachians, stethocanthids, and fragments of other forms), palaeoniscoid osteichthyans (including the predator *Tegeolepis*), various arthropods, and ammonoids (Feldmann and Hackathorn 1996). The arthropods, ammonoids, and placoderms were all free-swimming organisms with the shared character of a tough outer armor (cuticle, calcium carbonate or dermal bone), which had to be punctured and fractured before the flesh underneath could be consumed. The Devonian sharks and palaeoniscoids were relatively small (*Tegeolepis* was amongst the largest, reaching 1.8 m), free-swimming species that were likely prey items for *Dunkleosteus* (Janvier 1996). Consuming these mobile and often hard prey would have required both capture speed and bite force, for which the feeding system of *Dunkleosteus*, with its high forces and high KT values, appears particularly well suited. The combination of power and speed seen in *Dunkleosteus* would have allowed it potentially to consume virtually all other aquatic species, making it one of the first true apex predators seen in the vertebrate fossil record.

Conclusions

This paper reports the development of a computer model of the skull and thoracic shield of *Dunkleosteus terrelli* along with a wide range of simulations of the cranial kinematics and bite forces during feeding of this large Devonian predator.

1. Results suggest that a four-bar-linkage is a valid hypothesis for the dynamics of feed-

ing in *Dunkleosteus*. The linkage system and simulation of physiologically typical amounts of cranial muscle contraction produced realistic measures of cranial and jaw rotation, as well as muscle strains comparable to those in modern fishes.

2. The maximum gape angle for *Dunkleosteus* is estimated to be approximately 45°. The main restriction for gape angle was the structure of the adductor muscles relative to the jaw joint, rather than the closing of the nuchal gap, which had been previously suggested to limit gape.
3. Kinematic transmission values calculated for the five skulls fall above the KT values of a different linkage system measured in modern fishes, and in the upper end of the range of hyoid linkage system values for modern groups. These high KT values coupled with a large volume expansion within the oral cavity as the cranium is lifted may have been able to produce pressure gradients capable of creating suction forces.
4. Mechanical advantage of the lower jaw was high in *Dunkleosteus*, similar to high MAs found in some modern biting fishes, indicating high force transmission from muscle to the bite point.
5. Bite force estimates of over 6000 N at the jaw tip and over 7000 N at the rear blade edge place *Dunkleosteus* as one of the most powerful biters on record. This value is greater than for any living group except great white sharks and certain alligators. However, it falls either above or in line with the bite force/size regression done by Huber et al (2005), depending on the assumed maximum muscle stress used, indicating that the large bite forces are a product of large size and efficient force transmission not only through the jaw and skull levers, but through the linkage system as well.
6. The high KT value coupled with the blade-like occlusal surface and large ''fang'' on the jaw tip indicates a potential lifestyle of capturing fast evasive prey, possibly other placoderms. The high bite forces show that *Dunkleosteus* also had the capability to fragment hard prey. This combination of fast skull kinematics and forceful jaw lever mechanics points toward predation on evasive free-swimming and armored prey, such as arthropods, ammonoids, and other placoderms.

Acknowledgments

The authors would like to thank M. LaBarbera, M. Coates, D. Jablonski, and S. Kidwell for reviewing early drafts of this manuscript; R. Blob and one anonymous reviewer for many helpful and thoughtful suggestions on the manuscript; G. Jackson and the Cleveland Museum of Natural History for providing access to the *Dunkleosteus* material; and W. Simpson, collections manager of vertebrate paleontology at the Field Museum of Natural History, Chicago, for granting access to the display specimen of *Dunkleosteus*. This work was funded by National Science Foundation grant DEB 0235307 to M. Westneat.

Literature Cited

Aerts, P., J. W. M. Osse, and W. Verraes. 1987. Model of jaw depression during feeding in *Astatotilapia elegans* (Teleostei: Cichlidae): Mechanisms for energy storage and triggering. Journal of Morphology 194:85–109.

Alexander, R. M. 1989. Mechanics of fossil vertebrates. Journal of the Geological Society, London 146:41–52.

———. 1996. Optima for animals, 2d ed. Princeton University Press, Princeton, N.J.

Allis, E. P. 1923. The cranial anatomy of *Chlamydoselachus anguineus*. Acta Zoologica 4:123–221.

Anderson, P. S. L. 2008. Cranial muscle homology across modern gnathostomes. Biological Journal of the Linnean Society 94:195–216.

Anderson, P. S. L., and M. LaBarbera. 2008. Functional consequences of tooth design: effects of blade shape on energetics of cutting. Journal of Experimental Biology 211:3619–3626.

Anderson, P. S. L., and M. W. Westneat. 2007. Feeding mechanics and bite force modelling of the skull of *Dunkleosteus terrelli*, an ancient apex predator. Biology Letters 3:76–79.

Anker, G. C. 1974. Morphology and kinetics of the stickleback, *Gasterosteus aculeatus*. Transactions of the Zoological Society, London 32:311–416.

Ashley-Ross, M. A., and G. B. Gillis 2002. A brief history of vertebrate functional morphology. Integrative and Comparative Biology 42:183–189.

Barel, C. D. N. 1983. Toward a constructional morphology of cichlid fishes (Teleostei, Perciformes). Netherlands Journal of Zoology 33:357–424.

Bellwood, D. R. 2003. Origins and escalation of herbivory in fishes: A functional perspective. Paleobiology 29:71–83.

Benton, M. J. 2005. Vertebrate Palaeontology. Blackwell, Oxford.

Binder, W. J., and B. V. Van Valkenburgh. 2000. Development of bite strength and feeding behavior in juvenile spotted hyenas (*Crocuta crocuta*). Journal of Zoology 252:273–283.

Blob, R. W. 1998. Mechanics of nonparasagittal locomotion in *Alligator* and *Iguana*: functional implications for the evolution of nonsprawling posture in the Therapsida. Ph.D. dissertation. University of Chicago, Chicago.

———. 2001. Evolution of hindlimb posture in nonmammalian

therapsids: biomechanical tests of paleontological hypotheses. Paleobiology 27:14–38.

Blob, R. W., and A. A. Biewener 1999. In vivo locomotor strain in the hindlimb bones of *Alligator mississippiensis* and *Iguana iguana*: implications for the evolution of limb bone safety factor and nonsprawling limb posture. Journal of Experimental Biology 202:1023–1046.

———. 2001. Mechanics of limb bone loading during terrestrial locomotion in the green iguana (*Iguana iguana*) and American alligator (*Alligator mississippiensis*). Journal of Experimental Biology 204:1099–1122.

Bone, Q., I. A. Johnston, A. Pulsford, and K. P. Ryan. 1986. Contractile properties and ultrastructure of three types of muscle fiber in the dogfish myotome. Journal of Muscle Research and Cell Motility 7:47–56.

Brazeau, M. D. 2009. The braincase and jaws of a Devonian ''acanthodian'' and modern gnathostome origins. Nature (in press).

Carr, R. K. 1995. Placoderm diversity and evolution. *In* M. Arsenault, H. Lelievre, and P. Janvier, eds. Studies on early vertebrates. (VIIth International Symposium, 1991, Miguasha Parc, Quebec.) Bulletin du Museum National d'Histoire Naturelle, Paris, 4e série, C 17(1–4):85–125.

Carroll, A. M., P. C. Wainwright, S. H. Huskey, D. C. Collar, and R. G. Turingan. 2004. Morphology predicts suction feeding performance in centrarchid fishes. Journal of Experimental Biology 207:3873–3881.

Coates, M. I., and S. E. K. Sequeira. 1998. The braincase of a primitive shark. Transactions of the Royal Society of Edinburgh (Earth Sciences) 89:63–85.

Cowan, R. 1975. 'Flapping valves' in brachiopods. Lethaia 8:23–29.

———. 1979. Functional Morphology. Pp. 487–489 *in* R. Fairbridge and D. Jablonski, eds. Encyclopedia of paleontology. Dowden, Hutchinson, and Ross, Stroudsburg, Penn.

Curtin, N. A., and R. C. Woledge. 1988. Power output and force-velocity relationship of live fibres from white myotomal muscle of the dogfish, *Scyliorhinus canicula*. Journal of Experimental. Biology 140:187–197.

DeMar, R. E. 1976. Functional morphological models: evolutionary and non-evolutionary. Fieldiana (Geology) 33:339–354.

Denison, R. H. 1978. Placodermi. Part. 2 of H.-P. Schultze, ed. Handbook of paleoichthyology. Gustav Fischer, Stuttgart.

Durie, C. J., and R. G. Turingan. 2004. The effects of opercular linkage disruption on prey capture kinematics in the teleost fish *Sarotherodon melanotheron*. Journal of Experimental Zoology 30:642–653.

Erickson, G. M., S. D. Van Kirk, J. Su, M. E. Levenston, W. E. Caler, and D. R. Carter. 1996. Bite-force estimation for *Tyrannosaurus rex* from tooth-marked bones. Nature 382:706–708.

Erickson, G. M., A. K. Lappin, and K. A. Vliet. 2003. The ontogeny of bite-force performance in American alligator (*Alligator mississippiensis*). Journal of Zoology 260:317–327.

Feldmann, R. M., and M. Hackathorn. 1996. Fossils of Ohio. Ohio Geological Survey Bulletin 70.

Ferry-Graham, L. A., and G. V. Lauder. 2001. Aquatic prey capture in ray-finned fishes: a century of progress and new directions. Journal of Morphology 248:99–119.

Gatesy, S. M., and D. B. Baier. 2005. The origin of the avian flight stroke: a kinematic and kinetic perspective. Paleobiology 31: 382–399.

Gaudin, T. J., M. T. Carrano, R. W. Blob, and J. R. Wible. 2006. Introduction. Pp. 1–17 *in* M. T Carrano, T. J. Gaudin, R. W. Blob, and J. R. Wible, eds. Amniote paleobiology. University of Chicago Press, Chicago.

Goujet, D. 2001. Placoderms and basal gnathostome apomorphies. *In* P. E. Ahlberg, ed. Major events in early vertebrate evolution: palaeontology, phylogeny, genetics and development. Systematics Association Special Volume 61:209–222. Taylor and Francis, London.

Gould, S. J. 2002. The structure of evolutionary theory. Harvard University Press, Cambridge.

Gould, S. J., and R. C. Lewontin. 1979. The spandrels of San Marco and the Panglossian paradigm: a critique of the adaptationist programme. Proceedings of the Royal Society of London B 205:581–598.

Gross, W. 1967. Uber das gebiss der Acanthodier und Placodermen. Journal of the Linnean Society (Zoology) 47:121–130.

Huber, D. R., T. G. Eason, R. E. Hueter, and P. J. Motta. 2005. Analysis of the bite force and mechanical design of the feeding mechanism of the durophagous horn shark *Heterodontus francisci*. Journal of Experimental Biology 208:3553–3571.

Janvier, P. 1996. Early vertebrates. Clarendon, Oxford.

Johanson, Z. 2003. Placoderm branchial and hypobranchial muscle and origins in jawed vertebrates. Journal of Vertebrate Paleontology 23:735–749.

Kammerer, C. F., L. Grande, and M. W. Westneat. 2006. Comparative and developmental functional morphology of the jaws of living and fossil gars (Actinopterygii: Lepisosteidae). Journal of Morphology 267:1017–1031.

Labandeira, C. C. 1997. Insect mouthparts: ascertaining the paleobiology of insect feeding strategies. Annual Review of Ecology and Systematics 28:153–193.

Lauder, G. V. 1980. Evolution of the feeding mechanism in primitive actinopterygian fishes: a functional anatomical analysis of *Polypterus*, *Lepisosteus*, and *Amia*. Journal of Morphology 163:283–317.

———. 1995. On the inference of function from structure. Pp. 1–18 *in* Thomason 1995.

Lauder, G. V., and T. Prendergast. 1992. Kinematics of aquatic prey capture in the snapping turtle *Chelydra serpentina*. Journal of Experimental Biology 164:55–78.

Long, J. A. 1995. A new plourdosteid arthrodire from the upper Devonian Gogo formation of Western Australia. Palaeontology 38:39–62.

———. 1997. Ptyctodontid fishes (Vertebrata, Placodermi) from the Late Devonian Gogo Formation, Western Australia, with a revision of the European genus *Ctenurella* Orvig, 1960. Geodiversitas 19:515–555.

Lucas, P. W. 2004. Dental functional morphology: how teeth work. Cambridge University Press, Cambridge.

Medler, S. 2002. Comparative trends in shortening velocity and force production in skeletal muscles. American Journal of Physiology 283:R368–R378.

Miles, R. S. 1969. Features of placoderm diversification and the evolution of the Arthrodire feeding mechanism. Transactions of the Royal Society of Edinburgh 68:123–170.

Miles, R. S., and T. S. Westoll. 1968. The placoderm fish *Coccosteus cuspidatus* Miller ex Agassiz from the Middle old red Sandstone of Scotland, Part 1. Descriptive morphology. Transactions of the Royal Society of Edinburgh 67:373–476.

Motta, P. J., R. E. Hueter, T. C. Tricas, and A. P. Summers. 2002. Kinematic analysis of suction feeding in the nurse shark, *Ginglymostoma cirratum* (Orectolobiformes, Ginglymostomatidae). Copeia 2002:24–38.

Muller, M. 1987. Optimization principles applied to the mechanism of neurocranium levation and mouth bottom depression in bony fishes (Halecostomi). Journal of Theoretical Biology 126:343–368.

———. 1989. A quantitative theory of expected volume changes of the mouth during feeding in teleost fishes. Journal of Zoology 217:639–661.

Myhrvold, N. P., and P. J. Currie. 1997. Supersonic sauropods? Tail dynamics in the diplodocids. Paleobiology 23:393–409.

Newberry, J. S. 1873. Description of fossil fishes. Ohio Geological Survey Report 1(2):245–355.

Nigg, B. M. 1994. General comments about modeling. Pp. 367–379 *in* B. M. Nigg and W. Herzog, eds. Biomechanics of the musculo-skeletal system. Wiley, Chichester, U.K.

Niklas, K. J. 1994. Morphological evolution through complex domains of fitness. Proceedings of the National Academy of Sciences USA 91:6772–6779.

Padian, K. 1991. Pterosaurs: were they functional birds or functional bats? Pp. 145–160 *in* J. M. V. Rayner and R. J. Wootton, eds. Biomechanics in evolution (Society for Experimental Biology Seminar Series 36). Cambridge University Press, Cambridge.

Plotnick, R. E., and T. K. Baumiller. 2000. Invention by evolution: functional analysis in paleobiology. *In* D. H. Erwin and S. L. Wing, eds. Deep time: *Paleobiology*'s perspective. Paleobiology 26(Suppl. to No. 4):305–323.

Radinsky, L. B. 1987. The evolution of vertebrate design. University of Chicago Press, Chicago.

Ross, C. F. 1999. How to carry out functional morphology. Evolutionary Anthropology 7:217–222.

Rudwick, M. J. S. 1964. The inference of function from structure in fossils. British Journal for the Philosophy of Science 15:27–40.

Sanford, C. P. J., and P. C. Wainwright. 2002. Use of sonomicrometry demonstrates link between prey capture kinematics and suction pressure in largemouth bass. Journal of Experimental Biology 205:3445–3457.

Seilacher, A., and M. LaBarbera. 1995. Ammonites as Cartesian divers. Palaios 10:493–506.

Shockey, B. J., D. A. Croft, and F. Anaya. 2007. Analysis of function in the absence of extant functional homologues: a case study using mesotheriid notoungulates (Mammalia). Paleobiology 33:227–247.

Signor, P. W. 1982. Resolution of life habitats using multiple morphologic criteria: shell form and life habits in turritelliform gastropods. Paleobiology 8:378–388.

Stanley, S. M. 1970. Relation of shell form to life habits in the Bivalvia (Mollusca). Geological Society of America Memoir 125.

Thomason, J. J., ed. 1995. Functional morphology in vertebrate paleontology. Cambridge University Press, Cambridge.

Trinajstic, K. M., and M. Hazelton. 2007. Ontogeny, phenotypic variation and phylogenetic implications of arthrodires of the Gogo Formation, Western Australia. Journal of Vertebrate Paleontology 27:571–583.

Van Wassenbergh, S., A. Herrel, D. Adrians, and P. Aerts. 2004. Effects of jaw adductor hypertrophy on buccal expansions during feeding of air breathing catfishes (Teleostei, Claridae). Zoomorphology 123:81–93.

Vogel, S. 1998. Cats' paws and catapults. Norton, New York.

Wainwright, P. C., and B. A. Richard. 1995. Predicting patterns of prey use from morphology of fishes. Environmental Biology of Fishes 44:97–113.

Wainwright, P. C., D. R. Bellwood, M. W. Westneat, J. R. Grubich, and A. S. Hoey. 2004. A functional morphospace for labrid fishes: patterns of diversity in a complex biomechanical system. Biological Journal of the Linnean Society 82:1–25.

Wainwright, S. A., W. D. Biggs, J. D. Currey, and J. M. Gosline. 1976. Mechanical design in organisms. Princeton University Press, Princeton, N.J.

Weggelaar, C. W., D. R. Huber, and P. J. Motta. 2004. Scaling of bite force in the blacktip shark *Carcharhinus limbatus*. Integrative and Comparative Biology 44:662.

Weishampel, D. B. 1995. Fossils, function and phylogeny. Pp. 34–54 *in* Thomason 1995.

Westneat, M. W. 1990. Feeding mechanics of teleost fishes (Labridae): a test of four-bar linkage models. Journal of Morphology 205:269–295.

———. 1994. Transmission of force and velocity in the feeding mechanisms of labrid fishes (Teleostei, Perciformes). Zoomorphology 114:103–118.

———. 2003. A biomechanical model for analysis of muscle force, power output and lower jaw motion in fishes. Journal of Theoretical Biology 223:269–281.

———. 2004. Evolution of levers and linkages in the feeding mechanisms of fishes. Integrative and Comparative Biology 44:378–389.

———. 2006. Skull biomechanics and suction feeding in fishes. Pp. 29–76 *in* R. E. Shadwick and G. V. Lauder, eds. Fish biomechanics. Academic Press, San Diego.

Wilga, C. D., P. C. Wainwright, and P. J. Motta. 2000. Evolution of jaw depression mechanics in aquatic vertebrates: insights from Chondrichthyes. Biological Journal of the Linnean Society 71:165–185.

Witmer, L. M. 1995. The extant phylogenetic bracket and the importance of reconstructing soft tissues in fossils. Pp. 19–33 *in* Thomason 1995.

Wroe, S., C. McHenry, and J. Thomason. 2005. Bite club: comparative bite force in big biting mammals and the prediction of predatory behaviour in fossil taxa. Proceedings of the Royal Society of London B 272:619–625.

Wroe, S, D. R. Huber, M. Lowry, C. McHenry, K. Moreno, P. Clausen, T. L. Ferrara, E. Cunningham, M. N. Dean, and A. P. Summers. 2008. Three-dimensional computer analysis of white shark jaw mechanics: how hard can a great white bite? Journal of Zoology 276:336–342.

Zhu, M., and H.-P. Schultze. 2001. Interrelationships of basal osteichthyans. *In* P. E. Ahlberg, ed. Major events in early vertebrate evolution: palaeontology, phylogeny, genetics and development. Systematics Association Special Volume 61:289–314. Taylor and Francis, London.